2017 IEEE/RSJ International Conference on Intelligent Robots and Systems (IROS)
September 24–28, 2017, Vancouver, BC, Canada

Biped Walking Stabilization Based on Foot Placement Control Using Capture Point Feedback

Hyobin Jeong, Okkee Sim, Hyoin Bae, KangKyu Lee, Jaesung Oh and Jun-Ho Oh, *Member, IEEE*

***Abstract*—In this paper we introduce a biped foot placement controller based on capture point (CP) feedback control. This capture point feedback controller generates desired Zero Moment Point (ZMP) according to current capture point error. We call this desired ZMP as Control-ZMP (cZMP). Using this cZMP, we constructed (i) a disturbance adapting walking pattern generator, (ii) an ankle torque reference generator, (iii) a landing foot position adjustor and, (iv) a step time adjustor. By applying these controllers, the biped system becomes robust over uneven terrain and external pushing disturbances. We considered cZMP as a key indicator of bipedal walking stability. If the cZMP is within the support polygon, the robot will track the cZMP by using (i) and (ii). If the cZMP is outside of the support polygon, the robot will change footstep position and time by using (iii) and (iv) (COM pattern will be changed by (i) too). Capture point dynamics is described based on a linear inverted pendulum (LIP) model. The performance of the suggested control algorithm is validated in the Choreonoid simulator with a model of DRC-HUBO+ [11], [12].**

I. Introduction

One of the strategies to achieve robust biped walking is by using stable walking pattern and applying a stabilizing controller. Walking pattern generation has been studied widely. Most biped walking systems have a high COM position and a limited supporting polygon. It needs a dynamic simple model to solve the problem. The Linear Inverted Pendulum (LIP) model [6] and concept of Zero Moment Point (ZMP) [9] is used for generating a stable walking pattern. The COM trajectory can be calculated analytically with the ZMP expressed as a function [13], [14]. The most popular approach is preview controller that can generate stable COM pattern according to any prescribed ZMP trajectory [5].

To stabilize bipedal walking under the strong external disturbance or uneven terrain condition, foot placement control is inevitable. Stepping on uneven terrain needs contact control of swing foot, and this problem has been studied with various approaches [8], [15], [16]. The re-planning of the swing foot position is an important strategy to prevent falling due to strong perturbation. There are several foot placement controls based on preview control approach [17], [18], [19]. Another approach of foot placement is a method using orbital energy [20], [21]. By estimating COM velocity, total orbital energy can be calculated. A new foot step is determined to maintain the original. Recently, Optimization tool is being used for foot placement control. Feng et al used LIPM and QP (Quadratic Programming) method to optimize foot step position with fixed duration of the steps [22].

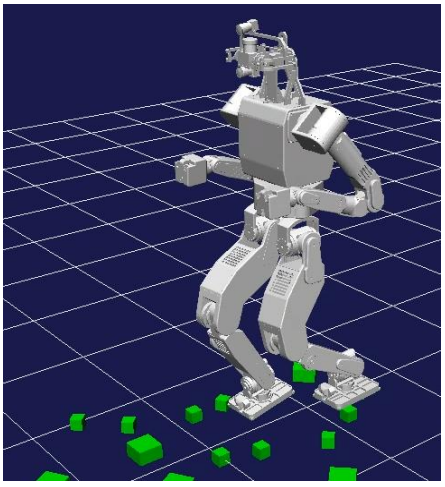

Fig. 1. Walking on uneven terrain with 2-cm blocks

The concept of capture point (CP) was introduced by Pratt et al. [4] and Hof [7] under different names—"Capture Point" and "Extrapolated Center of Mass"—respectively. In addition, Takenaka et al. [3] suggested "Divergent Component of Motion" as a new state of LIP dynamics. The main idea of all these concepts is basically the same as the stepping point on the floor in order to stop the robot completely. Foot placement control can be done by estimating the CP.

Englsberger et al. suggested the concept of CP control with ZMP. It can be used for not only gait generation, but real time CP controller [1]. The ZMP is not a control target, but it becomes a control output of the CP controller. Englsberger et al. has proposed a new view point of the LIP model, and its approach is investigated analytically. However, only ZMP control inside the supporting polygon and no foot placement was considered. We have utilized a part of this work; we constructed foot placement and step timing control strategies. In this paper, we will use the term "Capture Point" and will follow the notation (symbol as well) of [1].

II. LIP Based Capture Point Dynamics and Concept of Capture Point Control

Jun-Ho Oh is with the Humanoid Research Center, School of Mechanical, Aerospace & Systems Engineering, Department of Mechanical Engineering, Korea Advanced Institute of Science and Technology, 291 Daehak-ro, Yuseong-gu, Daejeon 305-338, Korea (e-mail: jhoh@kaist.ac.kr).

Hyobin Jeong, Okkee Sim, Hyoin Bae, KangKyu Lee and Jaesung Oh are with the Humanoid Research Center, School of Mechanical, Aerospace & Systems Engineering, Department of Mechanical Engineering, Korea Advanced Institute of Science and Technology. (e-mail: dhb111@kaist.ac.kr).

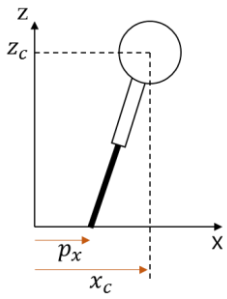

Fig. 2. Linear Inverted Pendulum Model

A. Brief introduction to LIP and Capture Point dynamics

In this section, we will briefly introduce the LIP model and derive the capture point. The LIP model is widely used for bipedal walking model because of its simplicity [1], [3], [5], [8]. The assumption of the LIP model is that the total mass is concentrated to one point at the COM and the COM moves along the plane with constant height [5], [6]. This assumption makes the LIP model linear and decoupled in each sagittal and lateral plane.

Fig. 1 shows LIP model in sagittal plane, where x_c is the position of the COM in the x direction and p_x is a moment-free point on the ground, which is the ZMP. The dynamics of this system can be expressed as

$$\ddot{x}_c = \omega^2 (x_c - p_x) . \quad (1)$$

Equation (1) is derived from the moment equilibrium equation at the point p_x, and ω is the system natural frequency expressed as $\sqrt{g / z_c}$. The LIP model is decoupled in x, y directions, so the descriptions of the y direction equations are equivalent with x direction.

The CP can be expressed as the position and velocity of the COM. There are several ways to derive the CP ([1], [3], [4], [7]), and we will omit the derivation here. CP, ξ_x, can be express as

$$\xi_x = x_c + \frac{\dot{x}_c}{\omega} . \quad (2)$$

By differentiating (2) and substituting (1), we can determine the dynamics between the CP and ZMP.

$$\dot{\xi}_x = \omega (\xi_x - p_x) . \quad (3)$$

From (1), (2), (3), we can derive the relationship between the COM, ZMP, and CP. With the given ZMP, COM diverges from ZMP, whereas the COM converges with the given CP. Similar to the COM, the CP is unstable with the given ZMP.

B. Concept of Capture Point Control

Many research studies considered only the COM and ZMP dynamics described by (1), and tried to achieve a stable COM trajectory for a given designed ZMP trajectory [5], [13], [14]. Englsberger suggested the concept of CP control from the natural dynamics of the CP. The main idea of CP control is to generate the ZMP that makes current CP achieve the target CP in given span of time; then, the COM will follow a stable CP trajectory. This concept of CP control can be used to for stable COM pattern generation or real-time CP feedback controller. In this section, we will briefly review CP end-of-step control (CPS) and CP tracking control (CPT), as suggested in [1].

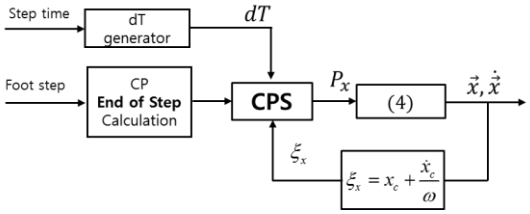

Fig. 3. COM position and velocity trajectory generation by CPS

If we solve the differential equation of (3) for a constant ZMP, the dynamics of CP in time domain can be derived as

$$\xi_x(t) = e^{\omega t} \xi_{x,0} + (1 - e^{\omega t}) p_x . \quad (4)$$

The CP exponentially shifts away from the initial CP along the line of CP and ZMP. If we assume ξ_x and $\xi_{x,0}$ as the target CP and current CP, respectively, and replace ξ_x, $\xi_{x,0}$, t by $\xi_{x,d}$, ξ_x, dT, it will lead to control law of CP.

$$p_x = \frac{\xi_{x,\mathrm{d}} - e^{\omega dT} \xi_x}{1 - e^{\omega dT}} = \frac{1}{1 - e^{\omega dT}} \xi_{x,\mathrm{d}} - \frac{e^{\omega dT}}{1 - e^{\omega dT}} \xi_x . \quad (5)$$

1) CP end-of-step control (CPS)

The main principle of CPS is to generate the ZMP from constant $\xi_{x,d}$ and varying dT. This constant $\xi_{x,d}$ is the CP end-of-step (ξ_{eos}), which can be obtained from future footstep position and time information. The method of calculation of $\xi_{x,eos}$ is introduced in [2]. In the actual application, dT is reset to t_{step} at the beginning of the step and decrease to $dT_{\min}$, which is bigger than zero. In case of current CP perturbation, CPS will generate the ZMP reference that makes current CP reach to $\xi_{x,eos}$.

2) CP tracking control (CPT)

Unlike CPS, the desired CP ($\xi_{x,d}$) of CPT is not constant, but dT is constant. We will call this dT as dT_{CPT}. Thus, CPT needs a predetermined CP trajectory to generate the reference ZMP. The current CP follows the desired CP with a time gap amount of dT_{CPT}, and if there is some perturbation on the current CP, CPT will try to stabilize the current CP by generating a new ZMP reference. We will call this ZMP as Control ZMP (cZMP). The stability and robustness of the control law (5) is validated analytically in [1].

III. Disturbance Adapting COM Pattern Generation using CPS and CPT

As mentioned previously, both CPS and CPT generate appropriate ZMP to stabilize the CP; however, CPS needs varying dT and CPT needs the trajectory of the target CP.

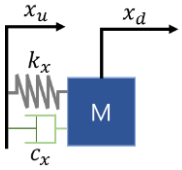

Fig. 4. Cartesian COM input model

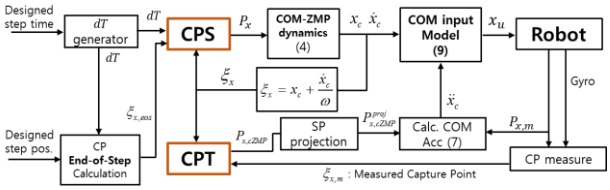

Fig. 5. Disturbance adapting COM pattern generator

CPS itself is not related to any future trajectory of footstep, so it is easy to modify future step position and step time. CPT showed more robust CP control performance than CPS in the experimental result in [1].

In this section, we will introduce a disturbance adapting COM pattern generation method using real-time feedback of the CP and ZMP. Disturbance adapting means that the COM pattern is modified in real time with respect to the CP and ZMP error, and its approach is combined with CPS and CPT. We will also use the second-order Cartesian COM input model. This model is a simple second-order model between input COM and output COM, which will be explained in this section. This pattern generation method has advantages of both CPS and CPT, which are simplicity and robustness.

A. *COM reference trajectory generation using CPS*

From the ZMP generated in CPS and (6), we can obtain the COM trajectory.

$$\begin{bmatrix} x_c(t) \\ \dot{x}_c(t) \end{bmatrix} = \begin{bmatrix} \cosh(\omega t) & \sinh(\omega t)/\omega \\ \omega \sinh(\omega t) & \cosh(\omega t) \end{bmatrix} \begin{bmatrix} x_{c,0} \\ \dot{x}_{c,0} \end{bmatrix} + \begin{bmatrix} 1-\cosh(\omega t) \\ -\omega \sinh(\omega t) \end{bmatrix} P_x \quad (6)$$

Despite COM-ZMP dynamics being originally unstable, the COM will be stable for given designed ZMP because the CP is controlled by CPS. The current CP for CPS feedback (ξ_x) is constructed from this COM position and velocity. It should be noted that this CP for CPS feedback is not the real CP of the robot but the internal variable to generate stable ZMP in CPS.

B. *Generate cZMP and desired COM acceleration using CPT*

We used the measured CP feedback in CPT to generate cZMP. For CPT, constant dT_{CPT} and predefined desired CP trajectory ($\xi_{x,d}$) is needed. In this study, without analytically calculating the CP trajectory, the output CP from CPS (ξ_x) was used for the desired CP trajectory, and the real measured (or estimated) CP of the robot was used for the CP feedback in CPT (COM and CP measurement is described in Appendix). The control law (5) will generate the cZMP according to the CP error.

This cZMP is a desired ZMP, which the humanoid is likely to have. However, there must be an error between the cZMP and the measured ZMP because of the multi-body effect or external disturbances. Englsberger et al. suggested position-based ZMP controller for the position-controlled robot [2]. This ZMP controller has a proportional feedback controller form constructed in [10], which is

$$\ddot{x}_d = k_f F_z / z_c (P_{x,m} - P_{x,cZMP}), \quad (7)$$

where $\ddot{x}_d$ is the desired COM acceleration and $P_{x,m}$ is the measured ZMP from the force-torque sensor. With the desired COM position and velocity from CPS and the desired COM acceleration from CPT, the final COM trajectory can be constructed.

C. *Combining CPS and CPT using the Cartesian COM input model*

In the previous section, we obtained the desired COM position, velocity, and acceleration. The COM position from CPS can be directly used for the COM pattern; however, it is not adaptable with external perturbation. Similarly, double integration of the desired COM acceleration can be used for the COM pattern, but the COM trajectory has the possibility to diverge; therefore, it is not suitable for COM pattern generation. To achieve both the benefits—disturbance adapting and stability—we used the Cartesian COM input model (Fig. 4).

Usually, a position-controlled robot controls the target joint angle to achieve Cartesian task such as the COM position or foot position based on inverse kinematics. However, there must exist joint deflections such that the real COM may not exactly follow our desired one. The Cartesian COM input model assumes that there is a spring and a damper between COM input and the real COM (Fig. 4). This assumption can be described as a simple second-order dynamic model.

$$M\ddot{x}_d + c_x \dot{x}_d + k_x x_d = c_x \dot{x}_u + k_x x_u . \quad (8)$$

Because we know $\ddot{x}_d$, $\dot{x}_d$, and x_d, we can obtain the value of the left-hand side of (8). Assume that this value is U, then we can calculate the input COM trajectory x_u in a discrete form as

$$x_u(k) = x_u(k-1) \cdot e^{-k/c \cdot dt} - U(e^{-k/c \cdot dt} - 1)/k , \quad (9)$$

where dt is the control period of the robot. Validation of this COM model is verified experimentally and its result is provided in Appendix.

Fig. 5 shows the overall structure of the disturbance adapting COM pattern generator. In the real application, CPT has time gap of dT_{CPT} from CPS (control time of CPS is faster than CPS by an amount of dT_{CPT}). Thus, the robot is synchronized with CPT's control time because CPT receives real time CP feedback.

IV. Foot Placement Control

Although our suggested COM pattern generator is adaptable to external disturbance, the robot cannot walk under

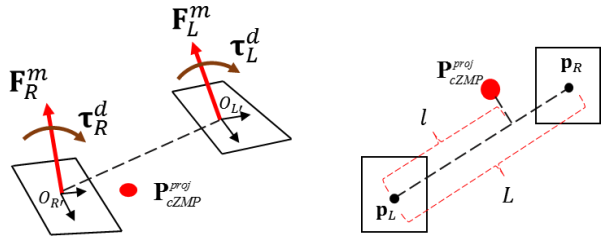

(a) Frame of each foot (b) ZMP distribution ratio

Fig. 6. ZMP distributor

strong perturbation or uneven terrain conditions. To achieve stable walking, foot placement control such as landing position, orientation, and timing control is critical. In this section, we will introduce the foot placement control by using the cZMP.

A. Landing orientation control with torque-controlled ankle

When the foot lands on the ground with the local slope, the robot will experience external disturbance, unless the foot adapts to the local slop quickly. Usually, the position-controlled robot controls the ankle with the desired roll-pitch angle; however, we will consider the robot with torque-controlled ankle joint here (we are in the process of building the ankle torque-controlled robot).

The cZMP can be used for the desired ankle torque according to the relationship between ZMP and ankle torque. During the single support phase (SSP), it is clear that cZMP and roll-pitch ankle torque are one to one mapping. Not like SSP, during the double support phase, mapping cZMP to ankle torque of both feet is an underdetermined problem. Therefore, we applied the concept of the ZMP distributor in [8]. First, we calculate total amount of ankle torque of both feet from the definition of the ZMP from (10).

$$\boldsymbol{\tau}_{total}^d = \boldsymbol{\tau}_R^d + \boldsymbol{\tau}_L^d = -(\mathbf{p}_R - \mathbf{P}_{cZMP}^{proj}) \times \mathbf{F}_R^m - (\mathbf{p}_L - \mathbf{P}_{cZMP}^{proj}) \times \mathbf{F}_L^m \quad (10)$$

$$\begin{cases} \boldsymbol{\tau}_R^d = \alpha \cdot \boldsymbol{\tau}_{total}^d \\ \boldsymbol{\tau}_L^d = (1-\alpha) \cdot \boldsymbol{\tau}_{total}^d \end{cases} \quad \left(\alpha = \frac{l}{L}\right), \quad (11)$$

$$\begin{bmatrix} \boldsymbol{\tau}_R^d \\ \boldsymbol{\tau}_L^d \end{bmatrix} \rightarrow \begin{bmatrix} {}^{R'}\boldsymbol{\tau}_R^d \\ {}^{L'}\boldsymbol{\tau}_L^d \end{bmatrix}, \quad (12)$$

where $\mathbf{F}_R^m$ and $\mathbf{F}_L^m$ are the measured force from the F/T sensor.

This total desired torque is distributed to each ankle torque according to (11). The α is a distribution ratio with the range of $0 \le \alpha \le 1$, and the rule of obtaining α is described in Fig. 6-(b). cZMP is projected to the line between center of both feet. The relative position of the projected point becomes α. After we determined $\boldsymbol{\tau}_R^d$ and $\boldsymbol{\tau}_L^d$, each desired torque can be transformed to coordinate of each foot, as in (12) (Fig. 6-(a)).

B. Landing foot position adjustor

The cZMP is continuously generated from the COM pattern generator, and this cZMP is usually in the inside of the supporting polygon. In case of strong perturbation, there will be large CP error and the cZMP will be generated outside of the supporting polygon. Then, it should be projected onto current supporting polygon because the ZMP cannot exist outside of the support polygon. However, if the cZMP projection occurs, the current CP of the robot will not reach the designed CP end-of step. From this idea, we set up the landing foot position control based on the cZMP projection. To determine the relationship between the cZMP projection and variation of CP end-of-step, the dynamics between the cZMP and CP end-of-step should be considered.

$$\boldsymbol{\xi}_{eos} = e^{\omega dT}\,\boldsymbol{\xi} + (1 - e^{\omega dT})\,\mathbf{P}_{cZMP}. \quad (13)$$

Equation (13) is vector form of (4) with different symbol, and we take partial derivative on (13) about $\mathbf{P}_{cZMP}$.

$$\mathbf{d}\boldsymbol{\xi}_{eos} = \frac{\partial \boldsymbol{\xi}_{eos}}{\partial \mathbf{P}_{cZMP}} \mathbf{dP}_{cZMP} = (1 - e^{\omega dT})\,\mathbf{dP}_{cZMP}, \quad (14)$$

$$\Delta\boldsymbol{\xi}_{eos} = \int \mathbf{d}\boldsymbol{\xi}_{eos}(t)\,dt. \quad (15)$$

If we regard $\mathbf{dP}_{cZMP}$ as the amount of cZMP projection in each axis, $\mathbf{d}\boldsymbol{\xi}_{eos}$ is the amount of change of CP end-of-step. It has the form of gain-varying proportional control. When dT is large (early stage of step), the cZMP projection leads the large change of the next step, and when dT is small, the cZMP projection has little effect on the next footstep. By integrating $\mathbf{d}\boldsymbol{\xi}_{eos}$ about time as in (15) and adding to the original landing foot position, we can obtain modified next foot position in real time. In real application, at the beginning of each step, $\Delta\boldsymbol{\xi}_{eos}$ should be initialized. The robot has kinematical range of foot, so the value of $\Delta\boldsymbol{\xi}_{eos}$ must be maintained in that range.

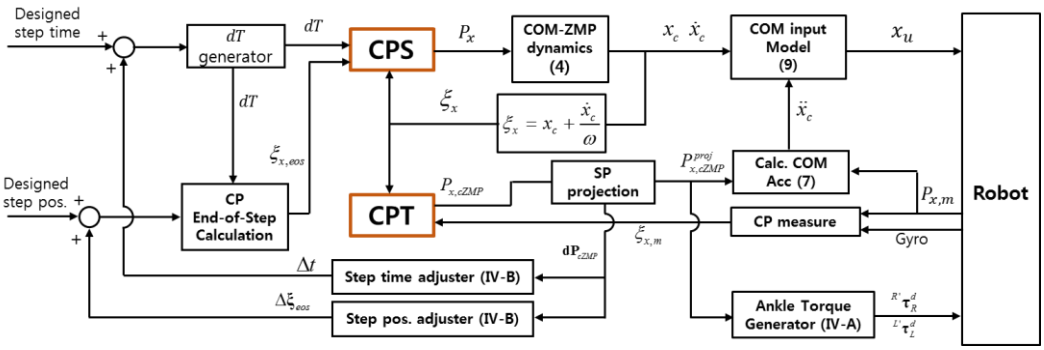

Fig. 7. Overall control block diagram.

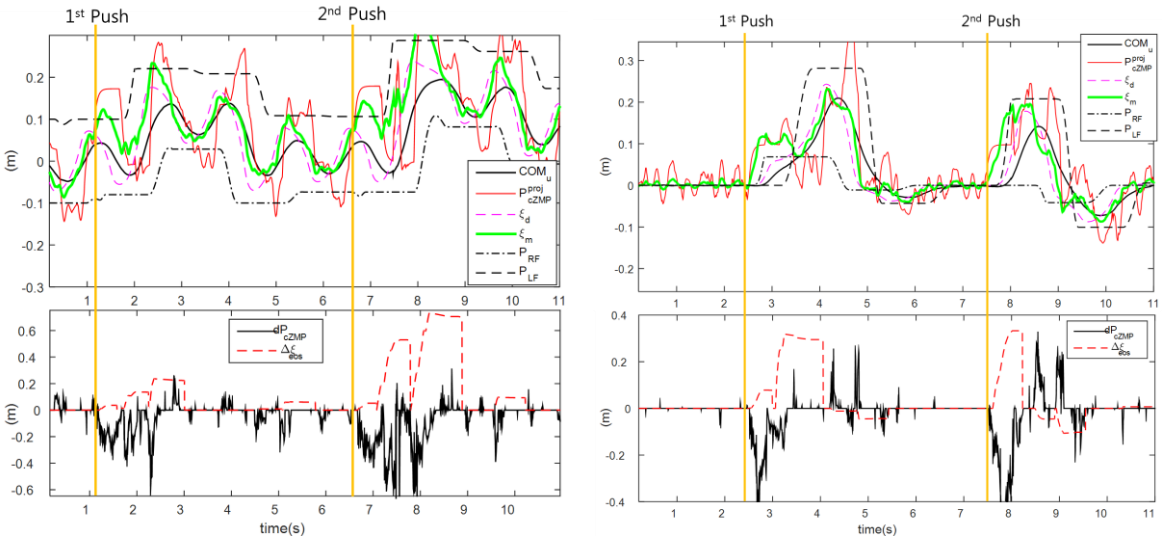

(a) Side push (b) Forward push

Fig. 8. Simulation data plot

C. *Step time adjustor*

Similar to the landing foot position adjustor, the cZMP projection can be used for the step time adjustor. To determine the relationship between the cZMP projection and step time, we took the p artial derivative of (13) about dT and $\mathbf{dP}_{cZMP}$.

$$\mathbf{d}\xi_{eos} = \frac{\partial \xi_{eos}}{\partial dT}\mathrm{d}(dT) + \frac{\partial \xi_{eos}}{\partial \mathbf{P}_{cZMP}}\mathbf{dP}_{cZMP}, \tag{16}$$

$$\mathbf{d}\xi_{eos} = (\xi - \mathbf{P}_{cZMP}^{proj})\,\omega \mathrm{e}^{\omega dT}\,\mathrm{d}(dT) + (1 - e^{\omega dT})\,\mathbf{dP}_{cZMP}. \tag{17}$$

We suppose that there is no change of CP end-of-step (i.e., $\mathbf{d}\xi_{eos} = \mathbf{0}$) even when the cZMP projection has occurred. From this assumption, we can obtain the appropriate change of dT.

$$\mathrm{d}(dT) = -\frac{1 - e^{\omega dT}}{\omega e^{\omega dT}} \cdot \frac{(\xi - \mathbf{P}_{cZMP}^{proj}) \circ \mathbf{dP}_{cZMP}}{\left\| (\xi - \mathbf{P}_{cZMP}^{proj}) \right\|^2}, \tag{18}$$

$$\Delta t = \int \mathrm{d}(dT)(\mathrm{t})\,\mathrm{dt}. \tag{19}$$

By integrating $\mathrm{d}(dT)$ about time as in (19), we can find the total amount of change of step time. In the real application, there must be minimum step time because of hardware limitation; therefore, $t_{step} + \Delta t$ cannot be smaller than the minimum step time. Not only that, if the remaining step time is less than the minimum step time, the step time cannot be shorter.

D. *Overall walking control scheme*

Fig. 7 shows the overall structure of biped walking control loop. We used the disturbance adapting COM pattern generator described in section Ⅲ. CPT continuously generates the cZMP according to the current CP error, and the cZMP is projected onto the supporting polygon. The projected cZMP is used to generate the desired COM acceleration and ankle torque generation. The amount of cZMP projection (i.e., $\mathbf{dP}_{cZMP}$) is used to adjust the step position and step time.

Although there can be many combinations of step time and step position satisfying (17), we give higher priority to step position change. That means we tried not to change the step position as much as possible. This is because in many humanoid walking situation such as stepping stone or narrow path situation, holding the designed step position is more important than changing step time. From this viewpoint, we constructed the step time adjustor with the assumption of no foot position change. However, there is a limitation of the step time change, so step position will also be changed.

V. SIMULATION RESULT

To demonstrate the effectiveness of our walking stabilizing algorithm, we performed the experiment using the Chorenoid simulator with the physical model of DRC-HUBO+ [11], [12]. The total body weight of simulated humanoid DRC-HUBO+ is 80 kg and total height is 170 cm. We performed the push experiment with certain impulse, and uneven terrain walking experiment with a randomly distributed 2-cm height block.

Fig. 8-(a) shows the result of lateral push experiment. While the robot is walking in place, it is pushed with an impulse of 30 Ns. Right after the robot is pushed, the cZMP is saturated in supporting polygon and $\mathbf{dP}_{cZMP}$ is generated. As depicted in Fig. 8-(a), $\Delta\xi_{eos}$ is produced and swing foot follows change of final landing position. Fig. 9-(a) is snapshot of simulation, which shows that the robot changes the landing position to maintain its balance.

In the second experiment, we push the robot in the sagittal direction with an impulse 20 Ns. While the robot is walking in place, it is pushed from the back, and the robot maintains its balance by taking a reactive step in forward direction. Fig. 8-(b) shows how the robot performed forward stepping. The sagittal cZMP immediately shifted to the toe of the robot and

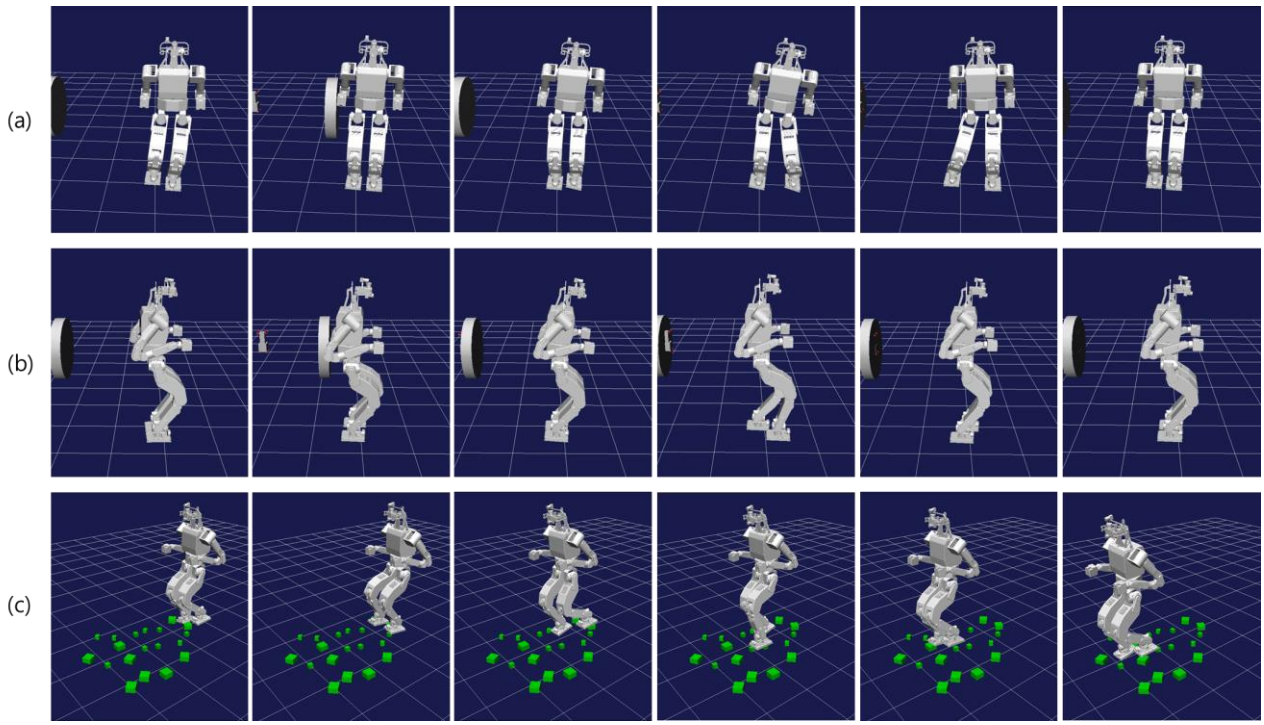

Fig. 9. Simulation snapshot (a) Side push, (b) Forward push, (c) walking on uneven terrain with 2-cm blocks

it saturated in the foot, and $\mathbf{dP}_{cZMP}$ is produced. Then, Δt and $\Delta\boldsymbol{\xi}_{eos}$ start to increase, making the swing foot move in the forward direction and the robot steps faster than the designed step time.

Fig. 9-(c) is the snapshot of the simulation that the robot walks through uneven terrain with 2-cm blocks. A 2-cm block can cause very stiff local slope depending on the contact point of the landing foot. Despite the steep local slope on the ground, our torque-controlled ankle and torque reference generator could adapt to uneven surface.

VI. Discussion and Future Work

Taking Capture Point (CP) into account, the Linear Inverted Pendulum (LIP) model provides a novel viewpoint of biped walking. Now the CP is the control target and from the CP controller with form of (5) produces an adequate target ZMP ([1], [2]). This concept had a decisive effect on our work; thus, based on this theory, our control algorithm could be constructed.

We described the methodology of balancing humanoid robots with various strategies. The first one involved disturbance-adapting COM pattern generator, which produced appropriate COM trajectories by using current CP. It not only generated COM trajectories, but also produced the desired ZMP (i.e., cZMP), which is used for foot placement control. We used this cZMP to produce an ankle torque reference. There is a certain advantage of controlling the ankle joint with torque instead of position. The robot can land on arbitrary local slope surface, and after landing, the foot can adapt to the surface having varying slope.

We thought that this cZMP is the key indicator of current walking stability. The current CP is reachable to CP end-of-step when the cZMP is in the supporting polygon. If the CP is outside the supporting polygon, the current CP will not be able to reach CP end-of-step and the next step must be modified. This idea is realized in the step time and position adjustors. By taking the partial derivative on simple CP dynamics (4), we could obtain the relationship between the cZMP projection, step time variation and CP end-of-step variation (Section Ⅳ-B, C).

It has been shown that the output of the step time adjustor and step position adjustor works well to balance the robot; however, sufficient proof has not been applied to its derivation. The formal analysis of both the adjustor and stability of time varying LIP system is a future work. In applying both adjustors, there should be a more precise rule between step time and step position changes under robotic constraints such as maximum joint specification and kinematical range, such that the robot can maximize its capacity for balancing itself.

To realize the result of simulation, we need a humanoid with a torque-controlled ankle joint. We are in the process of developing the hardware, and some experiments have been executed for examining the practicality of ankle-joint torque control. Through continued simulation, we are going study the appropriate specifications such as maximum torque and control bandwidth.

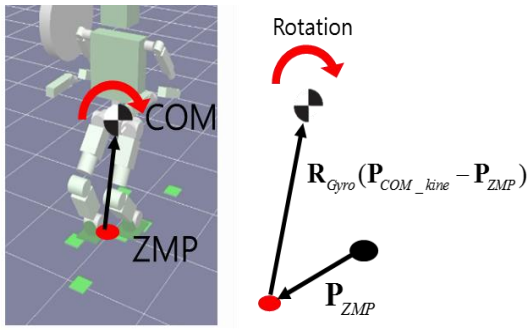

Fig. 10. The COM measurement

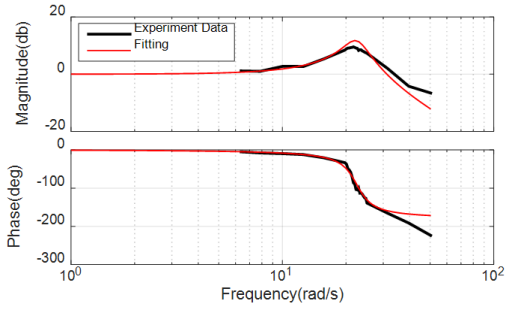

Fig. 11. Result of COM excitation experiment. Real data and model fiting

APPENDIX

1) COM measurement: In this study, The COM is measured by using measured ZMP and gyro angle. The robot has internal position of COM according to inverse kinematics. This COM is rotated around the measured ZMP as a pivot. It can be expressed as

$$\mathbf{P}_{COM\_m} = \mathbf{P}_{ZMP} + \mathbf{R}_{Gyro}(\mathbf{P}_{COM\_kine} - \mathbf{P}_{ZMP}) . \quad (20)$$

We obtained the velocity of the COM by numerical differentiation of (20)

2) Cartesian COM input model: Validity of this COM model can be investigated by the system identification experiment. We performed system identification by exciting the real robot (DRC-HUBO+) with a sinusoidal COM input and measured the real COM. We obtained a bode plot and a fit with the second-order model. In Fig. 11, experimental measurement of the bode plot is fitted with the second-order system. We can also find the model parameters by this COM excitation experiment.

ACKNOWLEDGMENTS

This work was supported by the Ministry of Trade, Industry and Energy(MOTIE, Korea) [Project Number: 10060103] .

REFERENCES

[1] Englsberger, Johannes, et al. "Bipedal walking control based on capture point dynamics." *Intelligent Robots and Systems (IROS), 2011 IEEE/RSJ International Conference on*. IEEE, 2011.

[2] Englsberger, Johannes, and Christian Ott. "Integration of vertical com motion and angular momentum in an extended capture point tracking controller for bipedal walking." Humanoid Robots (Humanoids), 2012 12th IEEE-RAS International Conference on. IEEE, 2012.

[3] Takenaka, Toru, Takashi Matsumoto, and Takahide Yoshiike. "Real time motion generation and control for biped robot-1 st report: Walking gait pattern generation." Intelligent Robots and Systems, 2009. IROS 2009. IEEE/RSJ International Conference on. IEEE, 2009.

[4] Pratt, Jerry, et al. "Capture point: A step toward humanoid push recovery." Humanoid Robots, 2006 6th IEEE-RAS International Conference on. IEEE, 2006.

[5] Kajita, Shuuji, et al. "Biped walking pattern generation by using preview control of zero-moment point." Robotics and Automation, 2003. Proceedings. ICRA'03. IEEE International Conference on. Vol. 2. IEEE, 2003.

[6] Kajita, Shuuji, et al. "The 3D Linear Inverted Pendulum Mode: A simple modeling for a biped walking pattern generation." Intelligent Robots and Systems, 2001. Proceedings. 2001 IEEE/RSJ *International* Conference on. Vol. 1. IEEE, 2001.

[7] Hof, At L. "The 'extrapolated center of mass' concept suggests a simple control of balance in walking." Human movement science 27.1 (2008): 112-125

[8] Kajita, Shuuji, et al. "Biped walking stabilization based on linear inverted pendulum tracking " Intelligent Robots and Systems (IROS), 2010 IEEE/RSJ International Conference on. IEEE, 2010.

[9] Vukobratović, Miomir, and J. Stepanenko. "On the stability of anthropomorphic systems." Mathematical biosciences 15.1-2 (1972): 1-37.

[10] Roy, Jaydeep, and Louis L. Whitcomb. "Adaptive force control of position/velocity controlled robots: theory and experiment." IEEE Transactions on Robotics and Automation 18.2 (2002): 121-137.

[11] Nakaoka, Shin'ichiro. "Choreonoid: Extensible virtual robot environment built on an integrated gui framework." System Integration (SII), 2012 IEEE/SICE International Symposium on. IEEE, 2012.

[12] Lim, Jeongsoo, et al. "Robot System of DRC- HUBO+ and Control Strategy of Team KAIST in DARPA Robotics Challenge Finals." Journal of Field Robotics 34.4 (2017): 802-829.

[13] Oh, Yonghwan, et al. "An analytical method to generate walking pattern of humanoid robot." IEEE Industrial Electronics, IECON 2006-32nd Annual Conference on. IEEE, 2006.

[14] Kim, Jung-Hoon. "Walking pattern generation of a biped walking robot using convolution sum." Humanoid Robots, 2007 7th IEEE-RAS International Conference on. IEEE, 2007.

[15] Ohashi, Eijiro, Tomoya Sato, and Kouhei Ohnishi. "A walking stabilization method based on environmental modes on each foot for biped robot." IEEE Transactions on industrial electronics 56.10 (2009): 3964-3974.

[16] Ma, Hongxu, Guang Li, and Jian Wang. "Humanoid walking pattern modification based on foot-ground equivalent contact control." Robotics and Biomimetics (ROBIO), 2009 IEEE International Conference on. IEEE, 2009.

[17] Urata, Junichi, et al. "Online decision of foot placement using singular LQ preview regulation." Humanoid Robots (Humanoids), 2011 11th IEEE-RAS International Conference on. IEEE, 2011.

[18] Nishiwaki, Koichi, and Satoshi Kagami. "Strategies for adjusting the zmp reference trajectory for maintaining balance in humanoid walking." Robotics and Automation (ICRA), 2010 IEEE International Conference on. IEEE, 2010.

[19] Morisawa, Mitsuharu, et al. "Reactive stepping to prevent falling for humanoids." Humanoid Robots, 2009. Humanoids 2009. 9th IEEE-RAS International Conference on. IEEE, 2009.

[20] Castano, Juan Alejandro, et al. "Dynamic and reactive walking for humanoid robots based on foot placement control." International Journal of Humanoid Robotics 13.02 (2016): 1550041.

[21] Stephens, Benjamin, and Christopher Atkeson. "Modeling and control of periodic humanoid balance using the linear biped model." Humanoid Robots, 2009. Humanoids 2009. 9th IEEE-RAS International Conference on. IEEE, 2009.

[22] Feng, Siyuan, et al. "Robust dynamic walking using online foot step optimization." Intelligent Robots and Systems (IROS), 2016 IEEE/RSJ International Conference on. IEEE, 2016.